

Article

Species-Specific Cuticular Phenotypes in Eutardigrada: A Morphometric Approach to Analyze the Variation of Star-Shaped Pores in *Minibiotus* Species

Alba Dueñas-Cedillo ^{1,2}, Jazmín García-Román ^{1,2}, Enrico Alejandro Ruiz ^{1,*} 
and Francisco Armendáriz-Toledano ^{2,*} 

- ¹ Laboratorio de Ecología, Departamento de Zoología, Escuela Nacional de Ciencias Biológicas, Instituto Politécnico Nacional, Prolongación de Carpio y Plan de Ayala S/N, Ciudad de México 11340, Mexico; aduenasc1600@alumno.ipn.mx (A.D.-C.); lgarcia0706@alumno.ipn.mx (J.G.-R.)
- ² Colección Nacional de Insectos, Departamento de Zoología, Instituto de Biología, Universidad Nacional Autónoma de México, Cto. Zona Deportiva S/N, C.U., Ciudad de México 04510, Mexico
- * Correspondence: eruizc@ipn.mx (E.A.R.); farmendariztoledano@ib.unam.mx (F.A.-T.)

Abstract: The use and characterization of cuticular attributes for separation and description of species has been traditionally used in heterotardigrades; however, despite that eutardigrades show structures in the cuticle with this potential use, the intra and interspecific variation of these characters using multivariate analysis (e.g., PCA, CVA) had not been analyzed. In this present study, the shape and size of the star-shaped pores of four *Minibiotus* species were analyzed under univariate and multivariate morphometric analysis of six morphological characters. Our approach to evaluate the variation of pores indicate the presence of species-specific cuticular phenotypes among *M. citlalium*, *M. constellatus*, *M. sidereus* and *M. pentannulatus*. The morphological differences in these elements of sculpture allowed us to acknowledge their range of variation, as well as the identification of new potential characters to recognize these taxa, which are included in a taxonomic key to identify them together with *M. eichhorni*, *M. pseudostellarus* and *M. vinciguerrae*.

Keywords: cuticle pore; multivariate analyses; morphometry; tardigrade sculpture



Citation: Dueñas-Cedillo, A.; García-Román, J.; Ruiz, E.A.; Armendáriz-Toledano, F. Species-Specific Cuticular Phenotypes in Eutardigrada: A Morphometric Approach to Analyze the Variation of Star-Shaped Pores in *Minibiotus* Species. *Diversity* **2021**, *13*, 307. <https://doi.org/10.3390/d13070307>

Academic Editor: Łukasz Kaczmarek

Received: 16 June 2021
Accepted: 2 July 2021
Published: 7 July 2021

Publisher's Note: MDPI stays neutral with regard to jurisdictional claims in published maps and institutional affiliations.



Copyright: © 2021 by the authors. Licensee MDPI, Basel, Switzerland. This article is an open access article distributed under the terms and conditions of the Creative Commons Attribution (CC BY) license (<https://creativecommons.org/licenses/by/4.0/>).

1. Introduction

The taxonomic identification process in tardigrades is a complex task, because many species display a low number of useful taxonomic characters and show a high range of phenotypic variation [1–5]. In species complexes, this situation is more evident. In some cases, the taxa do not have conspicuous qualitative traits for identification purposes (see, e.g., [3,6–8]). To cope with this, tardigrade taxonomists have proposed several morphological quantitative attributes to discriminate among species (see, e.g., [9–14]). Thus, the taxonomy of limno-terrestrial tardigrades is based on the analysis of both qualitative and quantitative characters [2,15–19].

Currently, systematic studies in this phylum are focused on clarify the taxonomy of species complexes, using predominantly morphological and morphometric characters supported by some genes, providing integrative approaches and much more robust species hypotheses [20–30].

The morphological attributes used in tardigrade taxonomy mainly consist of lineal measurements from body, bucco-pharyngeal apparatus and claws (see, e.g., [2,3,9,31–34]). Additionally, the relationship between a target structure with respects to the bucco-pharyngeal tube length, known as the *pt* index, is considered [9]. The methodological strategy to analyze these characters, either in their original scale or by means of *pt* indices, is based on the comparison of their variation intervals, such as the ranges and mean values of the problem specimens, or by choosing a single specimen of a similar body size to the one described as a typical in an earlier paper or original description [13].

In this sense, the variation of continuous traits has helped to reveal and separate species in the tardigrade classes Heterotardigrada [35,36] and Eutardigrada [37,38]. However, in some taxa that have a remarkable degree of morphological variation, the lineal measurements have not been informative enough to distinguish and separate species [39,40]. To solve this problem, more continuous characters standard protocols for comparison and multivariate analyses to support differences among tardigrade species have been incorporated (see, e.g., [11,16,17,41]). Furthermore, many structures in the descriptions and the proposal of protocols to compare morphometric characters (such as special TR templates in the form of MS Excel files [13]) have enhanced the taxonomic practice and facilitated species delimitation in tardigrades [33,42,43].

The use of continuous attributes in a multivariate context, along with geometric morphometric analyses, have improved the discriminatory power of the analysis of the characters to recognize cryptic species [36]. For example, the analysis of traditional morphometric variables by means of principal component analysis as well as the study of shape variation of claws and dorsal segmental plates using geometric morphometrics, allowed to separate morphs within the *Pseudechiniscus suillus* complex [36].

Another important contribution to tardigrade taxonomy is the addition of characters useful to the recognition of species, such as the description of shape, size and distribution of different cuticular elements (pores, gibbosities, plates, cirrus, dorsal sculpture, spurs on claws and dentate collars) [3,17,36,44,45]. However, the description and analysis of variation of these elements is mainly focused in Heterotardigrada [36,46], but poorly documented in Eutardigrada, even though numerous species mainly of *Macrobiotus hufelandi* group [3,42] and other genera as *Paramacrobiotus* [47] display different pores, granulation, and ornamentations on cuticle. This may be because, in some eutardigrades, these elements are not as conspicuous as in the case of heterotardigrades.

In the present study, we analyze the morphological variation of the cuticular elements of body surface from four *Minibiotus* species that display numerous pores with variable shapes (e.g., rounded multi-lobated and star-shaped on entire body, including the legs): *M. citlalium* Dueñas-Cedillo and García-Román, 2020, *M. constellatus* Michalczyk and Kaczmarek, 2003, *M. sidereus* Pilato et al., 2003 and *M. pentannulatus* Londoño et al., 2017. These species share a holotropical distribution in America and Africa. *Minibiotus constellatus* was described from Peru [48], *M. sidereus* described from Ecuador [49] and recorded from Mexico [50], *M. pentannulatus* described from Colombia [51] and recently recorded from Tanzania [27] and *M. citlalium* recently described from Mexico [50]. In the Iztaccíhuatl volcano, *M. citlalium* and *M. sidereus* were recorded in the same moss species and samples; therefore, they also share habitat characteristics [50].

Given the occurrence of star-shaped pores in the cuticle, *M. citlalium*, *M. constellatus*, *M. sidereus* and *M. pentannulatus* are similar to *M. pseudostellarus* Roszkowska, Stec, Ciobanu and Kaczmarek, 2016 and *M. eichhorni* Michalczyk and Kaczmarek, 2004, but they differ from the latter two species by the distribution pattern of this cuticular elements. The star-shaped pores in *M. pseudostellarus* and in *M. eichhorni* are randomly distributed and arranged in six transverse rows, respectively [19,52]. However, in *M. citlalium*, *M. constellatus*, *M. sidereus* and *M. pentannulatus*, the star-shaped pores are distributed in 11 transverse rows. Furthermore, these four species display similar morphology of eggshells with ringed processes. The above characteristics support that these taxa conform a species-group, within the genus. Nonetheless, *M. citlalium* and *M. sidereus* are the most morphologically similar. Both species present larger stars in the anterior and posterior regions of the body, a larger pair of stars in the fourth pair of legs and a very similar eggshell [49,50].

Currently, there is a set of qualitative and quantitative characters to recognize these four species, namely the macroplicoid sequence, number and size of the star-shaped pores on the external surface of legs I–IV, granulation on the legs, egg size and number of annulations in egg ornamentation. However, the identification process of these taxa must be corroborated with egg morphology, since in the majority of the Macrobiotoids, the egg traits have more weight for identification purposes [3,27,42], although in most

cases, obtaining the egg is difficult. In fact, there is no description of *M. constellatus* and *M. pseudostellarus* eggs [19,48].

Therefore, based on the differences observed in the cuticular elements of body surface among *M. citlalium*, *M. constellatus*, *M. sidereus* and *M. pentannulatus* species, in this work, the shape and size of the star-shaped pores were analyzed under a univariate and multivariate morphometric approach. Our main objective was to evaluate if the morphological variation of these structures has been differentiated among these taxa, so they may provide additional useful characters for their identification. For this purpose, new quantitative and taxonomic traits from multi-lobated star-shaped pores are proposed, as well as a terminology and standardized morphometric measurements for their analyses. Our intention is not to test the species hypotheses of *Minibiotus* taxa, but rather to improve the discriminatory power of character analysis to recognize the members of these species group, with emphasis on the species that present the greatest morphological similarity and that coexist in sympatry in the same moss samples: *M. citlalium* and *M. sidereus*.

2. Material and Methods

The entire cuticle (including the legs) of *M. constellatus*, *M. sidereus*, *M. pentannulatus* and *M. citlalium* is smooth and exhibits numerous pores with variable shape, such as rounded (76 1 in [49]; Figures 5, 6 and 11–14 in [48]; Figure 3 in [51]; Figure 5a,b in [50]); multi-lobated (up to four tips) (Figure 1 in [49]; Figures 1, 2 and 11 in [48]; Figure 3 in [51]; Figure 5c,d in [50]) and star-shaped (five or six tips) (Figure 1 in [49]; Figures 1–4 and 11–14 in [48]; Figure 3 in [51]; Figure 5e,f in [50]). The morphological analysis of the cuticular elements on body surface in these species was only focused in multi-lobated and star-shaped pores distributed on the entire dorsal surface of body; hereinafter, we will refer to both types of ornamentations as pores.

Images of pores from four *Minibiotus* species were obtained from photographs of type series and specimens identified by the authors.

Photographs of *M. sidereus* were provided by Giovanni Pilato (2019) and were obtained by us directly from specimens collected in the Iztaccíhuatl volcano [50]; *M. citlalium* images were generated directly from the specimens, which integrate the type series reported in Dueñas-Cedillo et al. [50]; images of *M. constellatus* corresponding to type specimens were obtained from the original paper (Figures 7 and 11–14 in [48]) and provided by the authors of the species; images of *M. pentannulatus* were obtained from the original description (Figure 3 in [51]) and from the figures displayed in the most recent record of this species by Stec et al. [27] (Figures 9 and 10).

It is worth to mention that both *M. citlalium* and *M. sidereus* were recently found by Dueñas-Cedillo et al. [50] in the same moss samples in the Iztaccíhuatl volcano, including samples used in the description of *Minibiotus citlalium* and other different samples collected in the Iztaccíhuatl volcano; both species were abundant in these samples. Therefore, the number of specimens and images of pores of these species that were used in the present study was higher than that of *M. constellatus* and *M. pentannulatus*.

The images of hatched specimens corresponding to *M. citlalium* and *M. sidereus* from the Iztaccíhuatl volcano were obtained using a phase contrast microscopy (PCM) (ZEISS Axioskop with digital camera AxioCam ERC 55); for each specimen, images were recorded at successive focal depths and automatically combined into a single sharp image (i.e., focus stacking). From full body images of each specimen, the length of the buccal tube was measured, and the pores were numbered consecutively in an anteroposterior direction from left to right (Figure 1a).

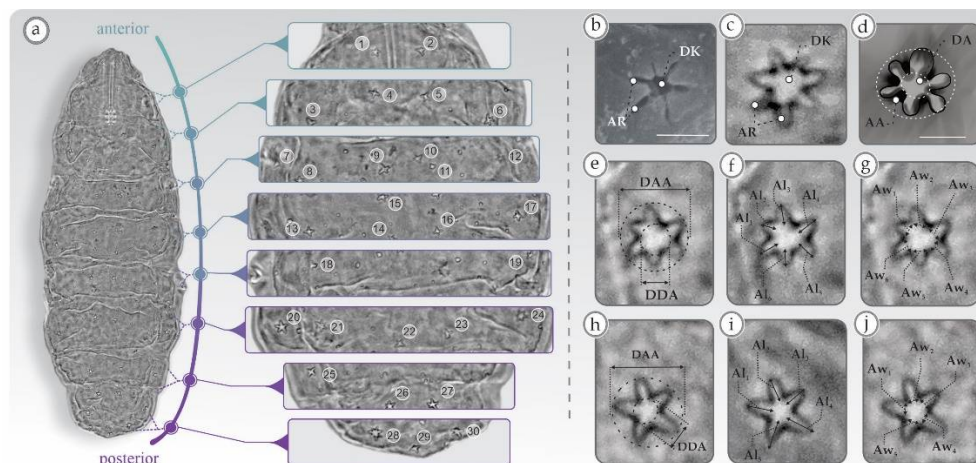


Figure 1. *Minibiotus sidereus*. Distribution and detail of the cuticular multi-lobate and star-shaped pores. (a) Dorsal habitus; (b–d) anatomy and areas of the multi-lobate and star-shaped pores; (e–j) morphological traits used to quantify the morphological variation of pores. AA: arm area, Al: arm length (Al₁: arm length one, Al₂: arm length two . . . Al₆: arm length six), Aw: arm width (Aw₁: arm width one, Aw₂: arm width two . . . Aw₆: arm width six), AR: arm, DAA: diameter of the arm area, DDA: diameter of the disk, DK: disc. The bar scales in (b,d) correspond to 2 μ m.

To analyze the morphological variation of the cuticular pores, the nomenclature used to describe the anatomy of sea stars was incorporated [53]. In the pores of *Minibiotus*, it was possible to recognize a central region called a disk, from which there are extensions that vary in number, from three to six, called arms (Figure 1b–d). Each pore was characterized by means of six morphometric traits as shown in the Figure 1e–j: (1) the diameter of the disc area (DDA) was measured as the diameter of the circumference that is formed by joining the base of the arms of pore (Figure 1e,h); (2) the diameter of the arm area (DAA) was measured as the diameter of the circumference that is formed by joining the apex of the arms of a pore (Figure 1e,h); (3) the proportion DAA/DDA was determined as the relation of the diameter of arm area respect to the diameter of the disc area; (4) the average arm length (AAL) was the average length of the arms of each pore, measured from the base (over the disc area) to the apex (over the arm area) of each arm (Figure 1f,i); (5) the average arm width (AAW) was the average width of the arms of each pore, measured at the base (over the disk area) of each arm (Figure 1g,j); (6) the proportion AAW/AAL, in relation of the average arm width with respect to the average arm length. In each trait, the *pt* index was calculated.

To facilitate the selection and measurement of these attributes, each pore was labeled with a number, and two circumferences were drawn to delimit both the diameter of the disc area and the diameter of the arm area (Figure 1a–d). The numbers and circumferences were established on the images of the complete specimens in the CorelDRAW Graphic Suite ver. 21.

The images of the specimens with the numbered pores and the marked circumferences in the pores were exported in “tiff” files for their measurement using the tps.Dig2 program ver. 2.31 [54]. In each specimen, pores were selected by means of random numbers for their measurement in micrometers. With the measurements of each star, a data matrix (Excel) was built.

A total of 145 pores were measured: in *M. constellatus* 44 pores from 1 specimen, in *M. sidereus* 44 pores from 8 specimens, in *M. pentannulatus* 33 pores from 1 specimen and in *M. citlalium* 24 pores from 4 specimens.

2.1. Data Analyses

Length in micrometers and *pt* values were obtained for each trait. The basic descriptive statistics were calculated (min, max, sum, variance, mean and standard deviation) and

the normality of the distribution for each of these attributes was independently tested by the Shapiro and Wilkinson's test [55]. The variation of each character was compared graphically among species by mean box plots. To evaluate the relative differences in the six attributes among taxa, a Guillaumin profile was calculated, with the difference of the means of each variable within each species and the total mean of each characteristic, divided by the total standard deviation of each species [56]. The differences among species in each trait were evaluated by means of ANOVA tests, from both lineal and *pt* values [57].

2.2. Effect of Size on the Morphometric Characters

The effect of size on morphometric characters in *M. citlalium* and *M. sidereus* was also evaluated, following the methodology proposed by Bartels et al. (2011) [58]. The relation of "body size", measured as the buccal tube length (BTL) with respect to the six continuous traits of pores was evaluated by means of linear regression per trait in each species. Regressions were performed from log-transformed values. The isometric or allometric trend was determined in each trait, comparing the slope with a slope of 1. To this end, we performed *t*-tests ($t = (b - 1)/SE$ of the slope) [57]. Regression analyses were carried out using PAST ver. 4.03 [59]. This analysis was not carried out in *M. constellatus* and *M. pentannulatus* because there was no sample size to compare the size of the body with respect to the pore characters.

2.3. Multivariate Analyses

To evaluate the main trends of morphological variation of pores within and among specimens and species, a Principal Component Analysis (PCA) was performed. Furthermore, a Canonical Variate Analysis (CVA) was included to determine to what extent these attributes explained the possible species differences [60].

In CVA analysis, multivariate differences among species were analyzed by means of both analysis of similarities (ANOSIM) and Pairwise Hotelling's T non-parametric tests. Both PCA and CVA were carried out independently from length (micrometers) and *pt* values of six characters respectively. Each pore was considered an operational taxonomic unit (OTU).

3. Results

3.1. Univariate Analyses

The basic descriptive statistics and results of normality test for each attribute in both micrometers and *pt* values are showed in the Tables 1 and 2. The ANOVA analysis of the six characters from micrometers and *pt* values supported significant differences in at least one comparison among species, the *pt* values are presented in italics (Figure 2; Tables 1 and 2).

The diameter of the disc area (DDA) was larger in *M. constellatus* ($1.94 \pm 0.03 \mu\text{m}$; 9.57 ± 0.17) and smaller in *M. pentannulatus* ($1.40 \pm 0.03 \mu\text{m}$; 7.49 ± 0.17), *M. sidereus* ($1.28 \pm 0.02 \mu\text{m}$; 4.70 ± 0.07) and *M. citlalium* ($1.24 \pm 0.25 \mu\text{m}$; 4.60 ± 0.17) (Figure 2, Table 1). Significant differences were found in the DDA among species ($\text{ANOVA}_{\text{linear}}$, $F_{3,134} = 109.3$, $p < 0.001$). The Tukey test showed differences in the following contrasts: *M. citlalium* vs. *M. constellatus* ($p < 0.001$), *M. citlalium* vs. *M. pentannulatus* ($p < 0.05$), *M. sidereus* vs. *M. constellatus* ($p < 0.001$), *M. sidereus* vs. *M. pentannulatus* ($p < 0.05$) and *M. constellatus* vs. *M. pentannulatus* ($p < 0.001$). Significant differences were also found between species from the *pt* values ($\text{ANOVA}_{\text{pt index}}$, $F_{3,134} = 259$, $p < 0.001$), in the same contrasts mentioned above (Table 2).

Based on the linear and *pt* index values, the diameter of the arm area (DAA) was larger in *M. constellatus* ($3.00 \pm 0.03 \mu\text{m}$; 14.74 ± 0.18), *M. sidereus* ($2.85 \pm 0.04 \mu\text{m}$; 10.51 ± 0.17) and *M. pentannulatus* ($2.62 \pm 0.05 \mu\text{m}$; 13.98 ± 0.29) and smaller in *M. citlalium* ($1.83 \pm 0.06 \mu\text{m}$; 6.79 ± 0.25) (Figure 2, Tables 1 and 2); significant differences were supported in the DDA among species ($\text{ANOVA}_{\text{linear}}$, $F_{3,134} = 90.21$, $p < 0.001$; $\text{ANOVA}_{\text{pt index}}$, $F_{3,134} = 227.1$, $p < 0.001$). The Tukey tests with linear values showed differences in the following contrasts: *M. citlalium* vs. *M. sidereus* ($p < 0.001$), *M. citlalium* vs. *M. pentannula-*

tus ($p < 0.05$), *M. citlalium* vs. *M. constellatus* ($p < 0.001$), *M. sidereus* vs. *M. pentannulatus* ($p < 0.05$) and *M. pentannulatus* vs. *M. constellatus* ($p < 0.001$). On the other hand, with *pt* index values, the Tukey test showed differences in the following contrasts: *M. citlalium* vs. *M. sidereus* ($p < 0.001$), *M. citlalium* vs. *M. pentannulatus* ($p < 0.05$), *M. citlalium* vs. *M. constellatus* ($p < 0.001$), *M. sidereus* vs. *M. pentannulatus* ($p < 0.05$) and *M. sidereus* vs. *M. constellatus* ($p < 0.001$) (Table 2).

Table 1. Morphological traits analyzed based on lineal measures from the pores from *M. citlalium*, *M. sidereus*, *M. pentannulatus* and *M. constellatus*, along with basic statistics, indicating the mean \pm SE, (min, max) and results of the ANOVA test (** significance value < 0.001); mean values with the same letter (superscript) did not differ statistically.

Trait	Species	Mean	F _{ANOVA}
Diameter of disc area (DDA)	<i>M. citlalium</i>	1.24 \pm 0.04; (0.9, 1.7) ^a	193 **
	<i>M. sidereus</i>	1.28 \pm 0.02; (1.0, 1.5) ^a	
	<i>M. pentannulatus</i>	1.40 \pm 0.03; (1.0, 1.7) ^b	
	<i>M. constellatus</i>	1.94 \pm 0.03; (1.4, 2.4) ^c	
Diameter of arm area (DAA)	<i>M. citlalium</i>	1.83 \pm 0.06; (1.3, 2.4) ^a	90.21 **
	<i>M. sidereus</i>	2.85 \pm 0.04; (2.3, 3.4) ^b	
	<i>M. pentannulatus</i>	2.62 \pm 0.05; (2.0, 3.2) ^c	
	<i>M. constellatus</i>	3.00 \pm 0.03; (2.4, 3.6) ^{b, d}	
DAA/DDA	<i>M. citlalium</i>	1.48 \pm 0.02; (1.3, 1.7) ^a	157.3 **
	<i>M. sidereus</i>	2.24 \pm 0.03; (1.8, 2.5) ^b	
	<i>M. pentannulatus</i>	1.87 \pm 0.02; (1.5, 2.2) ^c	
	<i>M. constellatus</i>	1.55 \pm 0.02; (1.2, 1.9) ^a	
Average arm length (AAL)	<i>M. citlalium</i>	0.36 \pm 0.008; (0.2, 0.4) ^a	6.62 **
	<i>M. sidereus</i>	0.57 \pm 0.05; (0.07, 1.0) ^b	
	<i>M. pentannulatus</i>	0.54 \pm 0.01; (0.3, 0.7) ^{c, b}	
	<i>M. constellatus</i>	0.46 \pm 0.02; (0.1, 0.76) ^{a, b}	
Average arm width (AAW)	<i>M. citlalium</i>	0.62 \pm 0.01; (0.4, 0.7) ^a	8.56 **
	<i>M. sidereus</i>	0.54 \pm 0.05; (0.07, 0.9) ^a	
	<i>M. pentannulatus</i>	0.64 \pm 0.01; (0.5, 0.7) ^a	
	<i>M. constellatus</i>	0.43 \pm 0.02; (0.4, 0.7) ^{a, b}	
AAW/AAL	<i>M. citlalium</i>	1.70 \pm 0.02; (1.5, 2.0) ^a	166.9 **
	<i>M. sidereus</i>	0.92 \pm 0.02; (0.7, 1.2) ^b	
	<i>M. pentannulatus</i>	1.20 \pm 0.03; (0.7, 1.6) ^c	
	<i>M. constellatus</i>	0.95 \pm 0.01; (0.7, 1.2) ^{b, d}	

The relationship between the diameter of the arm area with respect to the diameter of the disc area (DAA/DDA) was larger in *M. sidereus* (2.24 \pm 0.03) than in *M. pentannulatus* (1.87 \pm 0.02), *M. constellatus* (1.55 \pm 0.02) and *M. citlalium* (1.48 \pm 0.02) (Figure 2, Table 1). Significant differences were found in these traits among species based on linear measurements (ANOVA_{linear}, $F_{3, 133} = 157.8$, $p < 0.001$). The Tukey test showed differences in the following contrasts: *M. citlalium* vs. *M. sidereus* ($p < 0.001$), *M. citlalium* vs. *M. pentannulatus* ($p < 0.001$), *M. sidereus* vs. *M. pentannulatus* ($p < 0.001$), *M. sidereus* vs. *M. constellatus* ($p < 0.001$) and *M. pentannulatus* vs. *M. constellatus* ($p < 0.001$). With respect to the values of *pt*, DAA/DDA was larger in *M. pentannulatus* (10.04 \pm 0.15) than *M. sidereus* (8.24 \pm 0.13), *M. constellatus* (7.65 \pm 0.11) and *M. citlalium* (5.43 \pm 0.06); significant differences were found in the relationship DAA/DDA among species based on the *pt* index (ANOVA_{pt index}, $F_{3, 132} = 170.1$, $p < 0.001$). The Tukey test showed differences in the following contrasts: *M. citlalium* vs. *M. sidereus* ($p < 0.001$), *M. citlalium* vs. *M. pentannulatus* ($p < 0.05$), *M. citlalium* vs. *M. constellatus* ($p < 0.001$), *M. sidereus* vs. *M. pentannulatus* ($p < 0.05$) and *M. sidereus* vs. *M. constellatus* ($p < 0.001$) (Table 2).

Table 2. Analysis of morphological traits based on *pt* index from the pores of *M. citlalium*, *M. sidereus*, *M. pentannulatus* and *M. constellatus*, along with basic statistics, indicating the mean ± SE (min, max) and results of the ANOVA test (** significance value < 0.001); mean values with the same letter (superscript) did not differ statistically.

Trait	Species	Mean	F _{ANOVA}
Diameter of disc area (DDA)	<i>M. citlalium</i>	4.60 ± 0.17; (3.4, 6.6) ^a	259 **
	<i>M. sidereus</i>	4.70 ± 0.07; (3.9, 5.3) ^a	
	<i>M. pentannulatus</i>	7.49 ± 0.17; (5.6, 9.6) ^b	
	<i>M. constellatus</i>	9.57 ± 0.17; (7.0, 11.9) ^c	
Diameter of arm area (DAA)	<i>M. citlalium</i>	6.79 ± 0.25; (4.8, 9.08) ^a	227 **
	<i>M. sidereus</i>	10.51 ± 0.17; (8.6, 12.97) ^b	
	<i>M. pentannulatus</i>	13.98 ± 0.29; (10.94, 17.46) ^{c, e}	
	<i>M. constellatus</i>	14.74 ± 0.18; (11.97, 17.95) ^{d, e}	
DAA/DDA	<i>M. citlalium</i>	5.4 ± 0.06; (4.7, 6.3) ^a	170 **
	<i>M. sidereus</i>	8.24 ± 0.13; (6.7, 10.05) ^b	
	<i>M. pentannulatus</i>	10 ± 0.15; (8.3, 12.20) ^c	
	<i>M. constellatus</i>	7.65 ± 0.11; (6.04, 9.51) ^d	
Average arm length (AAL)	<i>M. citlalium</i>	1.33 ± 0.03; (0.97, 1.62) ^a	16.95 **
	<i>M. sidereus</i>	2.16 ± 0.21; (0.27, 3.9) ^b	
	<i>M. pentannulatus</i>	2.90 ± 0.08; (2.02, 4.03) ^c	
	<i>M. constellatus</i>	2.28 ± 0.12; (0.56, 3.75) ^{d, b}	
Average arm width (AAW)	<i>M. citlalium</i>	2.31 ± 0.06; (1.60, 2.74) ^a	21.72 **
	<i>M. sidereus</i>	2.03 ± 0.21; (0.24, 3.9) ^a	
	<i>M. pentannulatus</i>	3.42 ± 0.05; (2.70, 4.10) ^b	
	<i>M. constellatus</i>	2.16 ± 0.11; (0.69, 3.48) ^a	
AAW/AAL	<i>M. citlalium</i>	6.39 ± 0.11; (5.27, 7.46) ^a	135 **
	<i>M. sidereus</i>	3.25 ± 0.07; (2.55, 4.22) ^b	
	<i>M. pentannulatus</i>	6.42 ± 0.18; (4.06, 8.59) ^a	
	<i>M. constellatus</i>	4.69 ± 0.09; (3.49, 6.09) ^c	

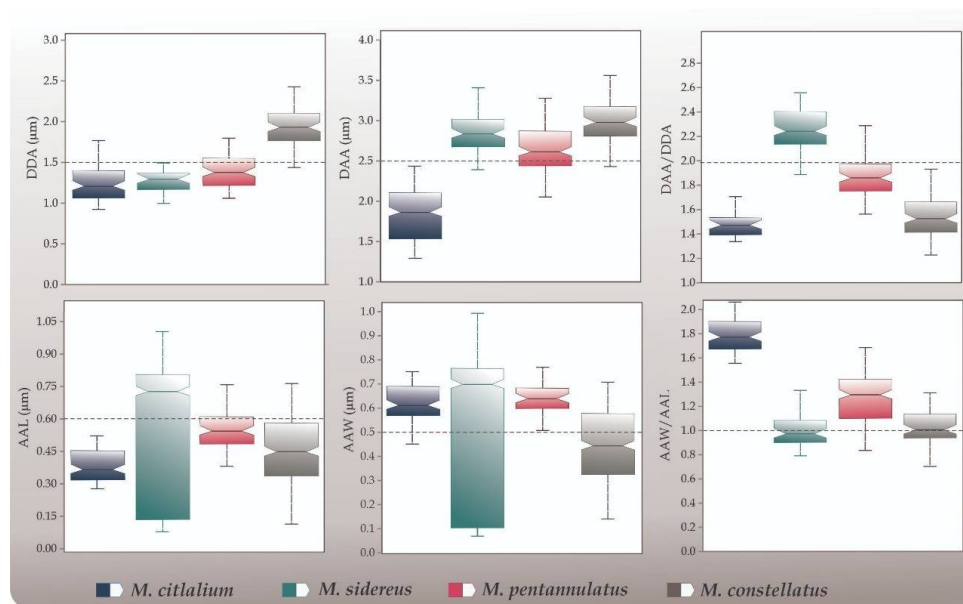


Figure 2. Box plots corresponding to the six characters used to quantify the morphological variation of pores among four *Minibiotus* species. DDA: diameter of disc area, DAA: diameter of the arm area, DAA/DDA: relationship between the diameter of the arms area with respect to the diameter of the disc area, AAL: average arm length, AAW: average arm width and AAW/AAL: relationship between the arm width average with respect to the arm length average.

The average arm length (AAL) was larger in *M. sidereus* ($0.57 \pm 0.05 \mu\text{m}$) than in *M. pentannulatus* ($0.54 \pm 0.01 \mu\text{m}$), *M. constellatus* ($0.46 \pm 0.02 \mu\text{m}$) and *M. citlalium* ($0.36 \pm 0.008 \mu\text{m}$), respectively (Figure 2, Table 1). Significant differences were found in the AAL among species (ANOVA_{linear}, $F_{3,133} = 6.62$, $p < 0.001$). The Tukey test indicated differences in the following contrasts: *M. citlalium* vs. *M. sidereus* ($p < 0.001$) and *M. citlalium* vs. *M. pentannulatus* ($p < 0.001$) (Table 1, Figure 2). The arm length average (AAL) from the *pt* values was larger in *M. pentannulatus* (2.90 ± 0.08) than in *M. constellatus* (2.28 ± 0.12), *M. sidereus* (2.16 ± 0.21) and *M. citlalium* (1.33 ± 0.03). Significant differences were found in the AAL *pt* values among species (ANOVA_{*pt* index}, $F_{3,133} = 16.95$, $p < 0.001$). The Tukey test showed differences in the following contrasts: *M. citlalium* vs. *M. sidereus* ($p < 0.05$), *M. citlalium* vs. *M. pentannulatus* ($p < 0.001$), *M. citlalium* vs. *M. constellatus* ($p < 0.001$), *M. sidereus* vs. *M. pentannulatus* ($p < 0.05$) and *M. pentannulatus* vs. *M. constellatus* ($p < 0.05$) (Table 2).

The arm width average (AAW) was larger in *M. pentannulatus* ($0.64 \pm 0.01 \mu\text{m}$) than in *M. citlalium* ($0.62 \pm 0.01 \mu\text{m}$), *M. sidereus* ($0.54 \pm 0.05 \mu\text{m}$) and *M. constellatus* ($0.43 \pm 0.02 \mu\text{m}$) (Figure 2, Table 1). Significant differences were found among species (ANOVA_{linear}, $F_{3,133} = 8.58$, $p < 0.001$). The Tukey test showed differences in the following contrasts: *M. citlalium* vs. *M. constellatus* ($p < 0.05$), *M. pentannulatus* vs. *M. constellatus* ($p < 0.05$) (Table 1, Figure 2). Respect to the AAW based in *pt* values, this proportion was larger in *M. pentannulatus* (3.42 ± 0.05) than in *M. citlalium* (2.31 ± 0.06), *M. constellatus* (2.16 ± 0.11) and *M. sidereus* (2.03 ± 0.21). Significant differences were found in the AAW among species (ANOVA_{*pt* index}, $F_{3,133} = 21.72$, $p < 0.001$). The Tukey test showed differences in the following contrasts: *M. citlalium* vs. *M. pentannulatus* ($p < 0.001$), *M. sidereus* vs. *M. pentannulatus* ($p < 0.001$) and *M. pentannulatus* vs. *M. constellatus* ($p < 0.001$) (Table 2).

The relationship between the arm width average with respect to the arm length average (AAW/AAL), was larger in *M. citlalium* (1.70 ± 0.02) than *M. pentannulatus* (1.20 ± 0.03), *M. constellatus* (0.95 ± 0.01) and *M. sidereus* (0.92 ± 0.02) (Figure 2, Table 1). Significant differences were found in the relationship AAW/AAL among species (ANOVA_{linear}, $F_{3,133} = 166.9$, $p < 0.001$). The Tukey test showed differences in the following contrasts: *M. citlalium* vs. *M. sidereus* ($p < 0.001$), *M. citlalium* vs. *M. pentannulatus* ($p < 0.001$), *M. citlalium* vs. *M. constellatus* ($p < 0.001$), *M. sidereus* vs. *M. pentannulatus* ($p < 0.001$) and *M. pentannulatus* vs. *M. constellatus* ($p < 0.001$) (Table 1, Figure 2). With respect to AAW/AAL based on the *pt* values, this proportion was smaller in *M. sidereus* (3.25 ± 0.07) than *M. pentannulatus* (6.42 ± 0.18). Significant differences were found in the AAW/AAL among species (ANOVA *pt* index, $F_{3,130} = 135.9$, $p < 0.001$). The Tukey test showed differences in the following contrasts: *M. citlalium* vs. *M. sidereus* ($p < 0.001$), *M. citlalium* vs. *M. constellatus* ($p < 0.001$), *M. sidereus* vs. *M. pentannulatus* ($p < 0.001$), *M. sidereus* vs. *M. constellatus* ($p < 0.001$) and *M. pentannulatus* vs. *M. constellatus* ($p < 0.001$) (Table 2).

The Guillaumin profile showed that the attributes with conspicuous differences among species were DDA, DAA, DAA/DDA and AAW/AAL (Figure 3).

Size Effect on the Characteristics

Linear regressions in *M. citlalium* showed that two traits of the star-shaped pores, average arm length (AAL) and average arm width (AAW) exhibit significant correlation with BTL (buccal tube length). The characters AAL, AAW and AAW/AAL were allometric (slope value significantly different from 1) respect to the buccal tube length (Supplementary Materials Table S1). Linear regressions in *M. sidereus* showed that three (AAL, AAW and AAW/AAL) out of the six continuous traits showed significant correlation with BTL (Supplementary Materials Table S2). The characters AL, AAW, AAW/AAL and DAA/DDA were allometric with respect to the buccal tube length (Supplementary Materials Table S2).

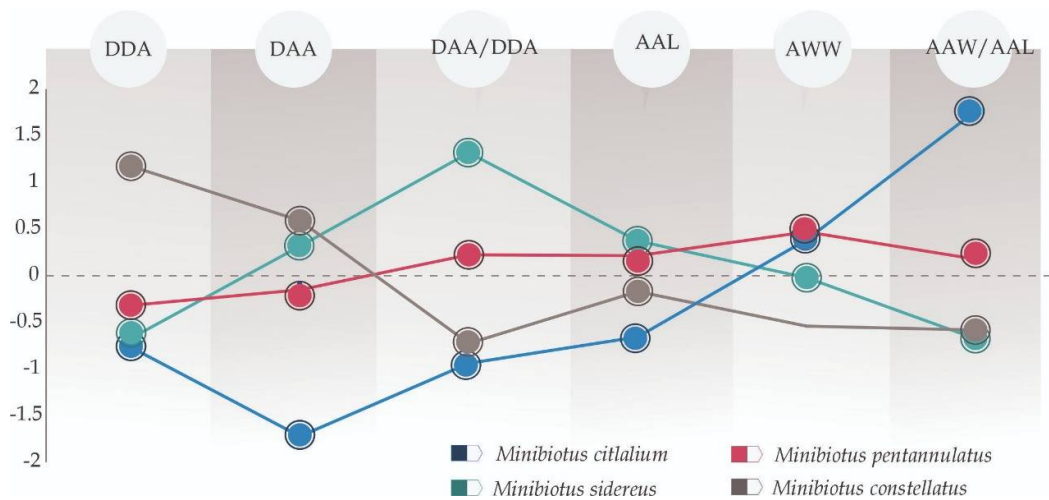


Figure 3. Guillaumin profile corresponding to the six characters used to quantify the morphological variation of pores of four *Minibiotus* species. For each variable, the points correspond to standardized mean differences among *Minibiotus* species. DDA: diameter of disc area, DAA: diameter of the arm area, DAA/DDA: relationship between the diameter of the arms area with respect to the diameter of the disc area, AAL: average arm length, AAW: average arm width, AAW/AAL: relationship between the arm width average with respect to the arm length average.

3.2. Multivariate Analyses

The PCA analysis of the linear measurements corresponding to the six characters explained 94.81% of the total variation in the first three principal components (PC1-57.05%; PC2-27.18%; and PC3-10.62%), while in the PCA of the *pt* indices of the six characters, the first three principal components together explained 95.38% of the total variation (PC1-69.87%; PC2-14.20%; and PC3-11.30%). In the corresponding three-dimensional scatter plots in both PCAs (linear measures and *pt* indexes in Figure 4a,b, respectively), the pores of the same specimen and species were closer in multivariate space, thus showing clusters of distinct phenotypes corresponding to the four species considered. Of these analyses, the one based on *pt* indices segregated the pore phenotypes into well-defined, discrete clusters, corresponding to each species (Figure 4b). In the analysis with linear measures, the morphological variables with larger contribution to explain the pattern were DDA, AAW and AAW/AAL (Figure 4a), while in the analysis with the *pt* index measures, the morphological variables with larger contribution to explain the pattern were DAA and AAW/AAL (Figure 4b).

Both CVA analyses using linear measurements and *pt* index explained 100% of the total variation in the first three canonical vectors (linear: CV1: 63.27%; CV2: 34.58%; CV3: 2.53%; *pt* indexes: CV1: 80.53%, CV2: 11.27%, CV3: 8.20%). In the CVA, using linear measurements, the discriminant function correctly classified 90.37% of the pores according to which species they belong. On the other hand, with the *pt* index, the discriminant function correctly classified 99.25% of the pores according to which species they belong. In both cases, the three-dimensional scatter plots grouped the pores in clusters corresponding to the species (Figure 5a,b). Only the scatter plot with the *pt* values showed the species in discrete clusters (Figure 5b). In the analysis with linear measures, the morphological variables that better explained the pattern were DAA, DDA, AAW and AAW/AAL (Figure 5a), while in the analysis with the *pt* index measures, the morphological variables that better explained the pattern were DAA, DDA and DAA/DDA (Figure 5b).

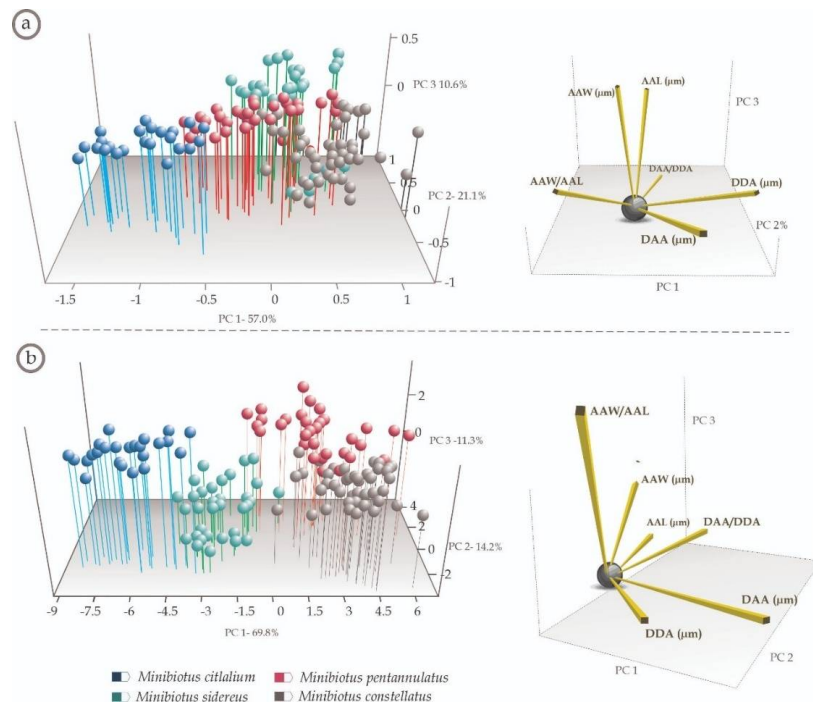


Figure 4. Principal Components Analyses with the six characters used to quantify the morphological variation of pores among four *Minibiotus* species. On the left, the scatter plot among the first three principal components. On the right, vectors corresponding to the contribution of each trait in multivariate space. (a) Analysis using micrometer values, (b) analysis using the *pt* values. DDA: diameter of disc area, DAA: diameter of the arm area, DAA/DDA: relationship between the diameter of the arm area with respect to the diameter of the disc area, AAL: average arm length, AAW: average arm width, AAW/AAL: relationship between the arm width average with respect to the arm length average.

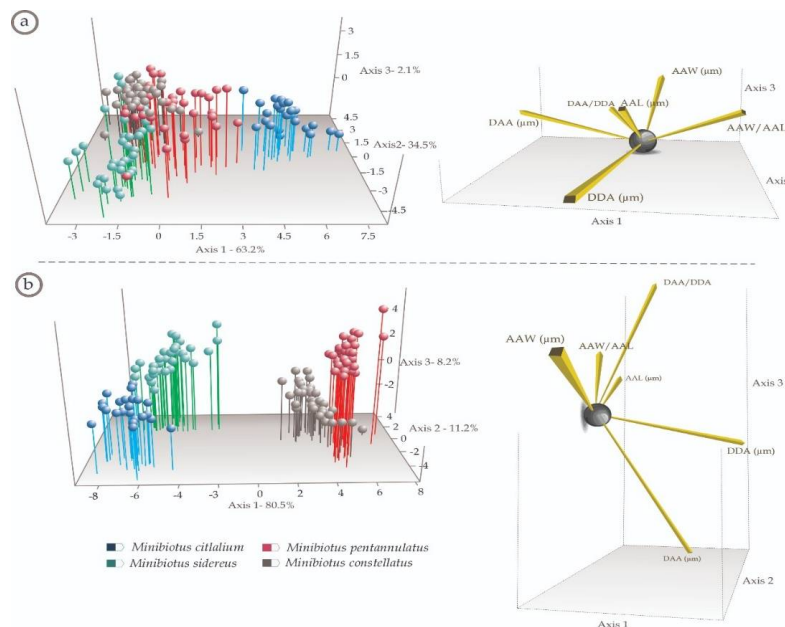


Figure 5. Canonical Variate Analyses with six characters used to quantify the morphological variation of pores among four *Minibiotus* species. On the left, scatter plot among first three canonical axes. On the right, vectors corresponding to the contribution of each trait in multivariate space. (a) Analysis using micrometer values, (b) analysis using the *pt* values. DDA: diameter of disc area, DAA: diameter of the arm area, DAA/DDA: relationship between the diameter of the arm area with respect to the diameter of the disc area, AAL: average arm length, AAW: average arm width, AAW/AAL: relationship between the arm width average with respect to the arm length average.

3.3. Dichotomous Key to the Species of *Minibiotus sidereus* Group

Minibiotus eichhorni, *M. pseudostellarus*, *M. vinciguerrae*, *M. sidereus*, *M. constellatus*, *M. pentannulatus* and *M. citlalium* are distinguished within the genus by the presence of rounded, multilobed and star-shaped pores on the dorsal cuticle. Therefore, based on these characters we present an illustrated dichotomous taxonomic key that improves the identification process of these species:

- 1 Star-shaped pores arranged in transverse rows on the dorsal cuticle (Figure 6) 2
- 1' Star-shaped pores randomly distributed on the dorsal cuticle (Figure 7) 3
- 2 Star-shaped pores on dorsal cuticle in 11 transverse rows (Figure 8a), which become double in the segments of the legs I–III (Figure 8b); a very large star-shaped pore (5–6 tips) on each leg of the fourth pair (Figure 8c) 4
- 2' Star-shaped pores on dorsal cuticle arranged in six transverse bands, not including larger groups of pores on frontal and caudal part of body (Figure 9) *M. eichhorni*
- 3 Presence of rounded, multilobated or star-shaped pores on cuticle (Figure 10a), macroplacoid length sequence $1 \leq 2 < 3$ (Figure 10b) and fine granulation only present on legs IV (Figure 10c) *M. pseudostellarus*
- 3' Presence of rounded, multilobated, star-shaped, and elliptical pores on cuticle, (Figure 11a), macroplacoid length sequence $1 > 2 < 3$ (Figure 11b), notable granulation and cuticular bars present on all legs (Figure 11c) *M. vinciguerrae*

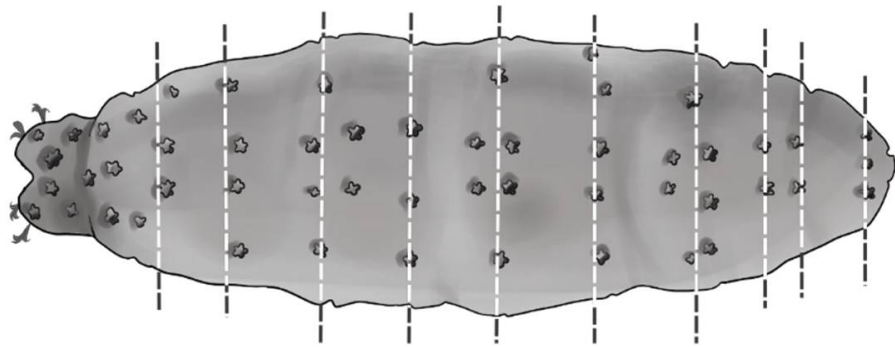


Figure 6. Dorsal habitus showing the star-shaped pores arranged in transverse rows (e.g., *Minibiotus constellatus*).

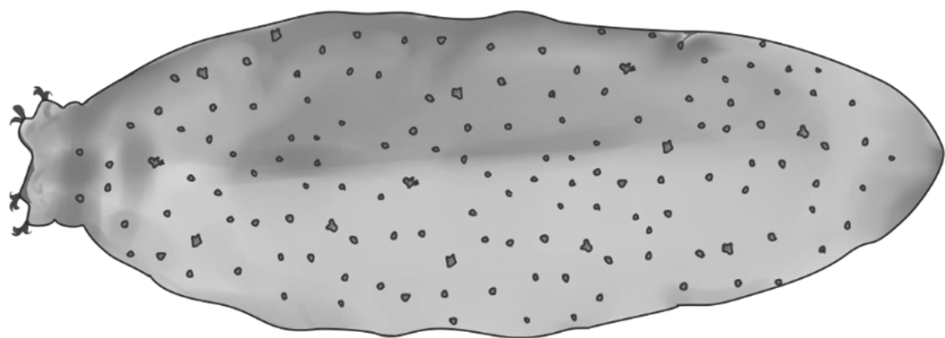


Figure 7. Dorsal habitus showing the star-shaped pores randomly distributed (e.g., *Minibiotus pseudostellarus*).

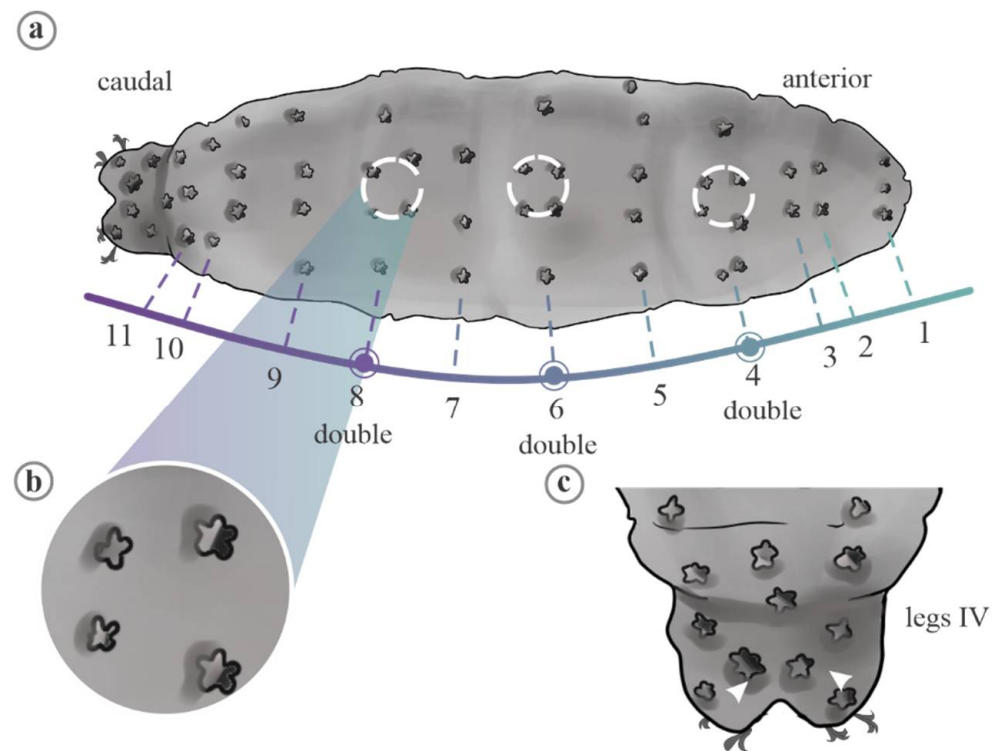


Figure 8. (a) Dorsal habitus showing the star-shaped pores arranged in 11 transverse rows (e.g., *Minibiotus constellatus*); (b) zoom of both rows of star-shaped pores; (c) caudal region, arrow heads indicate the very large star-shaped pores.

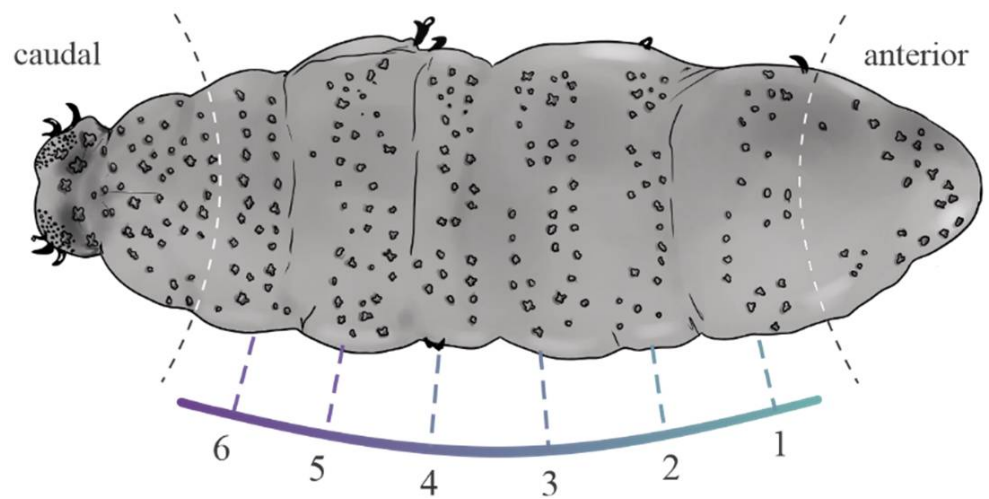


Figure 9. Dorsal habitus of the star-shaped pores arranged in six transverse bands (e.g., *Minibiotus eichhorni*).

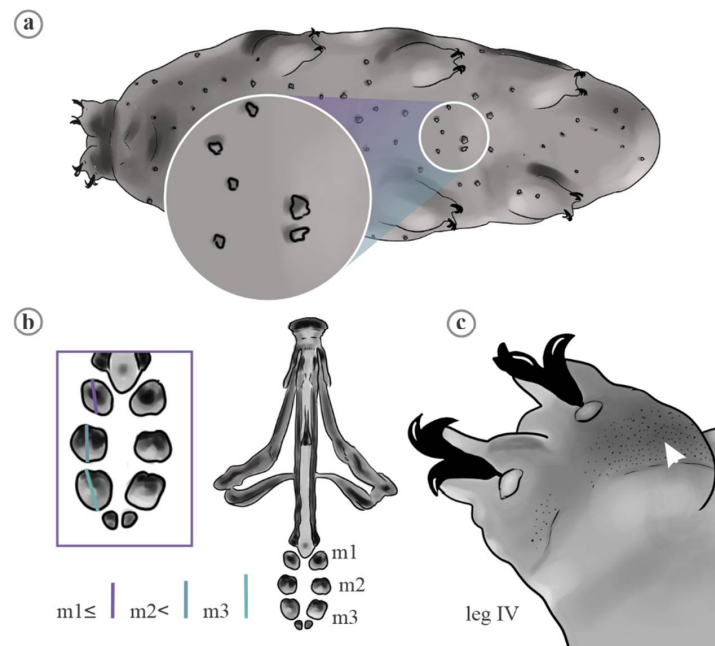


Figure 10. Detail of habitus, bucco-pharyngeal apparatus and legs of *Minibiotus pseudostellarus*. (a) Cuticle with rounded, multilobated or star-shaped pores; (b) bucco-pharyngeal apparatus; the purple, blue and green lines indicate the size of each placoid. m1: first macroplacoid, m2: second macroplacoid, m3: third macroplacoid; (c) legs IV; the arrow head indicates the fine granulation.

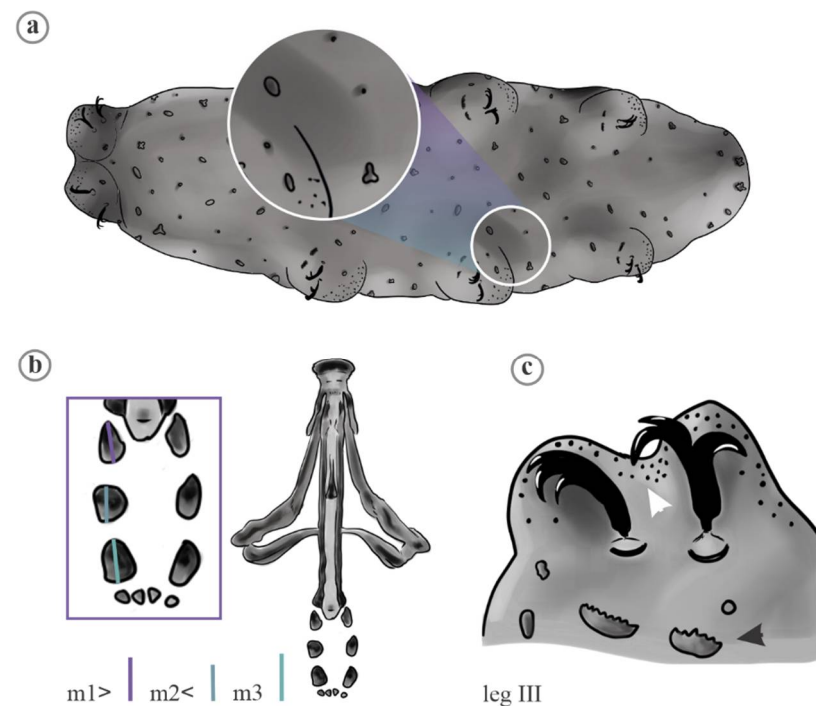


Figure 11. Detail of the ventral habitus, bucco-pharyngeal apparatus and legs of *Minibiotus vinciguerrae*. (a) Cuticle with rounded, multilobated, star-shaped and elliptical pores; (b) bucco-pharyngeal apparatus; the purple, blue and green lines indicate the size of each placoid. m1: first macroplacoid, m2: second macroplacoid, m3: third macroplacoid; (c) leg IV; the white arrow head indicates the notable granulation, the black arrow head indicates the cuticular bars.

4 The arms of the star-shaped pores are almost as wide as they are long (Figure 12), that is, the ratio between the average arm width respect to average arm length (AAW/AAL) is almost 1 5

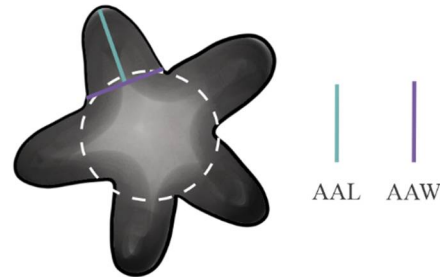


Figure 12. Relationship between the length and width of arms in the star-shaped pores (e.g., *Minibiotus sidereus* type). The green and purple lines indicate the length and width, respectively.

4' The length of the arms of the star-shaped pores are almost double than their width (Figure 13); thus, the ratio between the average arm width, respect to the average arm length (AAW/AAL) may quantify up to 2 6

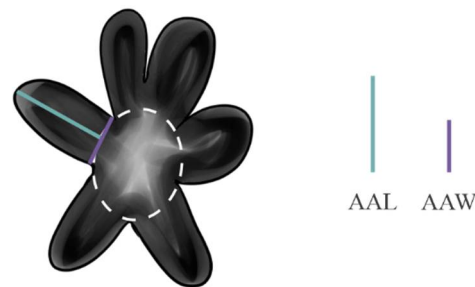


Figure 13. Relationship between the length and width of arms in the star-shaped pores (e.g., *Minibiotus citlalium* type). The green and purple lines indicate the length and width, respectively.

5 Presence of three star-shaped pores, two of them larger than the last one, on external view in legs I-III (Figure 14a), macroplacoid length sequence, $1 > 2 < 3$ (Figure 14b) *M. sidereus*.

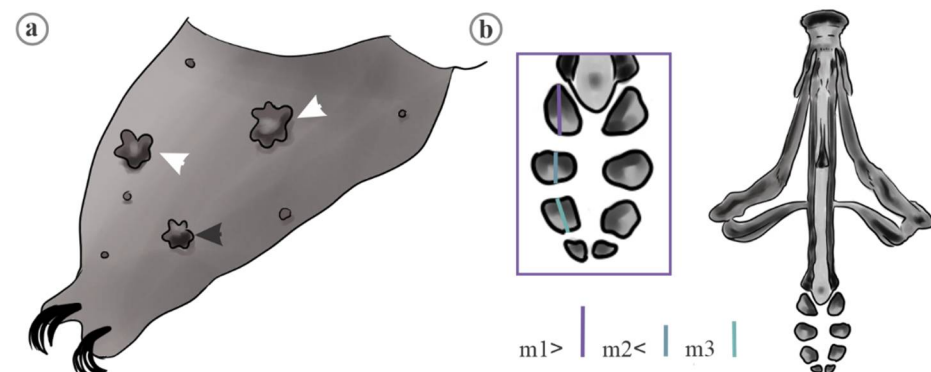


Figure 14. Detail of leg and bucco-pharyngeal apparatus of *Minibiotus sidereus*; (a) leg II with three star-shaped pores; white and black arrows indicate the large and small pores, respectively; (b) bucco-pharyngeal apparatus; the purple, blue and green lines indicate the size of each placoid. m1: first macroplacoid, m2: second macroplacoid, m3: third macroplacoid.

5' Presence of two star-shaped pores of similar size on external view in legs I-III (Figure 15a), macroplacoid length sequence, $1 > 2 > 3$ (Figure 15b) *M. constellatus*

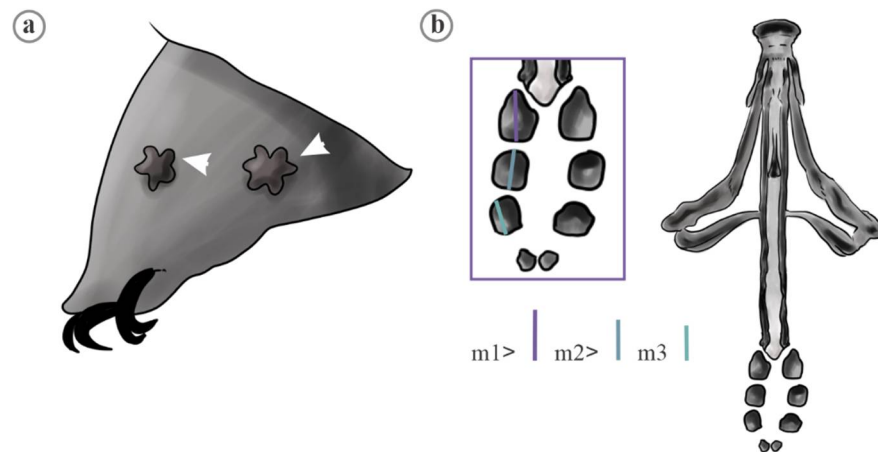


Figure 15. Detail of leg and bucco-pharyngeal apparatus of *Minibiotus constellatus*; (a) leg II with two star-shaped pores; white arrow head indicates pores of similar size; (b) bucco-pharyngeal apparatus; the purple, blue and green lines indicate the size of each placoid. m1: first macroplacoid, m2: second macroplacoid, m3: third macroplacoid.

6 Presence of two star-shaped pores, one of them conspicuously larger than the other one on external view in legs I-III (Figure 16a), macroplacoid length sequence, $1 > 2 = 3$, (Figure 16b) *M. citlalium*

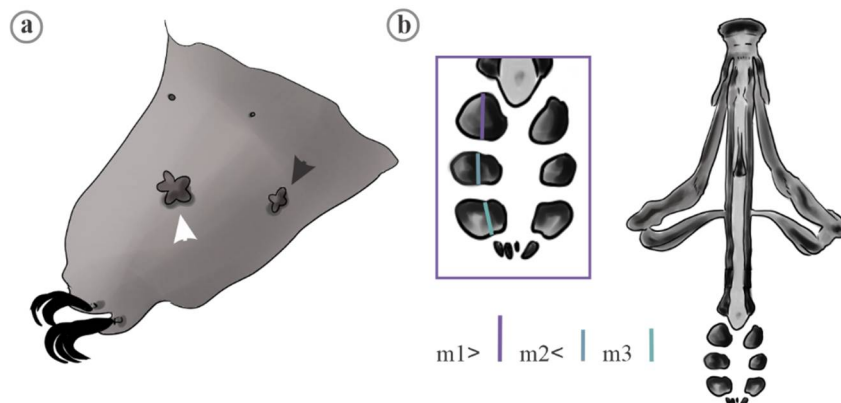


Figure 16. Detail of leg and bucco-pharyngeal apparatus of *Minibiotus citlalium*; (a) leg III with three star-shaped pores; white and black arrows indicate big and small pores, respectively; (b) bucco-pharyngeal apparatus; the purple, blue and green lines indicate the size of each placoid. m1: first macroplacoid, m2: second macroplacoid, m3: third macroplacoid.

6' Presence of three or four star-shaped pores on external view in legs I-III, one of them conspicuously larger than the other three, one of them surrounded by a patch of granulation (Figure 17a), macroplacoid length sequence, $1 > 2 < 3$ (Figure 17b) *M. pentannulatus*

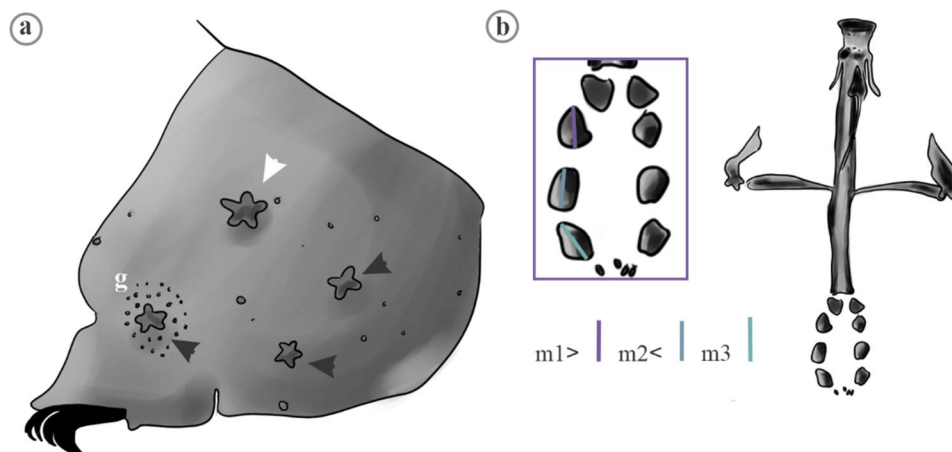


Figure 17. Detail of leg and bucco-pharyngeal apparatus of *Minibiotus pentannulatus*; (a) leg II with three star-shaped pores; white and black arrows indicate large and small pores, respectively; (b) bucco-pharyngeal apparatus; the purple, blue and green lines indicate the size of each placoid. g: patch of granulation, m1: first macroplacoid, m2: second macroplacoid, m3: third macroplacoid.

4. Discussion

The characterization of multi-lobated and star-shaped pores in *Minibiotus* species allowed us to acknowledge the range of variation of these cuticular elements and, by extension, the identification of new potential characters to recognize *M. citlalium*, *M. constellatus*, *M. sidereus* and *M. pentannulatus*. Our morphometric approach to evaluate the variation of pores suggest the occurrence of species-specific cuticular phenotypes in the *Minibiotus* species complex. The morphological differences in these elements of sculpture among *M. citlalium*, *M. constellatus*, *M. sidereus* and *M. pentannulatus* was supported by both univariate and multivariate analyses.

4.1. Characters Analyzed

The use and characterization of cuticular attributes for the separation and description of tardigrade species has been traditionally used in members of the Heterotardigrada and Eutardigrada [3,36,61–63]. In Heterotardigrada, the inclusion of different elements (e.g., cephalic papillae, scapular plates, projections from the plates and dorsal and ventral sculpture given by the presence of striae and punctuations, among others) have provided, in some cases, important features for taxonomy and systematics studies [63,64]. The recognition of lineages in Heterotardigrada by means of molecular markers have proven highly congruent with cuticular attributes, as phylogenies in accordance with the taxa delimited with these types of characters have been recovered [65–67]. In addition, the evolution of cuticular elements in Heterotardigrada is consistent with the diversification of both deeply divergent and more recent lineages, which is reflected in the occurrence of diagnostic attributes at different levels of the taxonomic scale in this group [68]. Furthermore, the intra- and interspecific analyses of the variation of cuticular elements via multivariate morphometric approaches supports that these characters are discriminatively powerful, allowing the recognition of infra-specific entities in Heterotardigrada [36].

Cuticular features in Eutardigrada have also been included in the descriptions and separation of taxa, although less frequently than in Heterotardigrada. For example, in some taxa of Hypsibioidea, Isohypsibioidea and Macrobiotioidea, diverse cuticular sculptural elements, such as reticulation, tubercles, gibbossites, punctures, granules, pores, papillae, spines and folds, are taxonomically useful [1,3,63,68,69]. The description of cuticular traits has provided useful information in phylogenetic studies, supporting different evolutionary lines, corresponding to supra-specific taxa [70,71]. At the specific level, qualitative and quantitative characters have been proposed for the description and recognition of some members of Eutardigrada [3,7,72]; however, although cuticular traits in Eutardigrades have

recently been used in descriptions and phylogenetic analyses, until now, the intra- and interspecific variation of these characters in a multi-variate context, has not been analyzed in this group to discriminating purposes, such as multi-lobate and star-shaped pores in the *Minibiotus* species evaluated in the present study.

Analyses of variance of six continuous traits (DDA, DAA, DAA/DDA, AAL, AAW and AAW/AAL) from cuticular pores among *M. citlalium*, *M. constellatus*, *M. sidereus* and *M. pentannulatus* showed that all of them were useful for separating these species. Based on these attributes, DDA, DAA and AAW/AAL could be used to identify to *M. citlalium* and *M. constellatus*, because their values display low overlapping among the remaining species. *Minibiotus citlalium* quantified the lowest diameter of arm area, and the highest ratio values between the width and length of arms, displaying smaller pores with arms until they are two times longer than wide. On the other hand, *M. constellatus* showed higher values of diameter of disc area. Despite that, *M. sidereus* and *M. pentannulatus* did not show discrete distributions in any characters, these taxa showed the highest values of DAA/DDA, displaying pores with arm area two times higher than disc area; thus, they can be identified from *M. citlalium* and *M. constellatus*. The interspecific variation patterns of DAA/DDA must be highlighted, because this proportion was statistically different among all studied taxa. This characteristic revealed that the star-shaped pores of each species have a different ratio. Thus, to improve identification, this attribute could be included in the description of the species with this sculpturing pattern. In addition, these characters are very easy to measure, and with a very simple methodology, the specific differences can be observed. The standardized characteristic means indicate that the whole set of attributes are useful for the taxonomy of these species, since each taxon has a unique combination of measures that allows their recognition.

4.2. Multivariate Analyses (Species-Specific Cuticular Phenotypes)

PCA of the quantitative characters showed that cuticular pores in these *Minibiotus* species display conspicuous morphological differences (Figures 4 and 5). These analyses also showed that *M. citlalium*, *M. constellatus*, *M. sidereus* and *M. pentannulatus* display strongly differentiated cuticular phenotypes, because the PCA's from six quantitative characters were consistent with the recovery of discrete groups corresponding to the analyzed taxa. Robustness of these clusters was demonstrated when axes that minimize the ratio of between-species and within species variation were produced in CVA, which did not disrupt the original distribution of pores corresponding to each species and display these cuticular elements in corresponding clusters. Multivariate analysis has been used extensively to identify and delimit morphological characters within and between species in several invertebrate taxa [73–75].

4.3. Effect of Size in Traits and *pt* Values

In Eutardigrada taxonomy, many continuous traits display correlations with body size [39,58,76]. A considerably proportion of these characters tends to grow proportionally with this trait (i.e., isometric traits), while in others, the growth is not proportional (i.e., allometric ones). The linear regressions in each species showed specific traits with allometric growth, and therefore, it is not suitable for *pt* indices. This agrees with the report by Bartels et al. [58], who showed a high number of qualitative characters with allometric growth.

The discriminating ability of *pt* indexes were outstanding. In the four species studied, the values of these indexes showed a decrease in intraspecific variability and an increase in interspecific variability. The discriminating capacity of the *pt* indices was outstanding, since in both the multivariate and univariate analyses, the differences between species were maximized, particularly in the multivariate analyses, allowing the recognition of discrete groups and a higher percentage of correct classification of the star-shaped pores according to the species to which they belong. These results fully confirm what was stated

by Pilato et al. [76], who described the usefulness of the *pt* index values, especially by showing a rather limited intraspecific variability between two Macrobiotidae species.

5. Conclusions

This study proposes new cuticular traits for the separation of species and their use in the identification of the members of the *Minibiotus sidereus* group, as well as other tardigrade species that display this type of cuticular ornamentation. From a simple and widely used methodology in other groups of animals, the intra- and interspecific variation of cuticular structures can be analyzed and the discriminatory ability can be put to test for delimitation purposes. Finally, a taxonomic key based on both discrete and continuous characters including those that describe morphological variation cuticular pores, is proposed.

Supplementary Materials: The supplementary materials are available online at <https://www.mdpi.com/article/10.3390/d13070307/s1>, Table S1. Linear regression of all morphometric traits measured of the star-shaped pored of *Minibiotus citlalium* in relation to buccal tube length (BTL). Data log–log transformed. N = sample size, b = slope, a * = intercept, r^2 = coefficient of correlation, $t = (b - 1)/SE$ of b, p = probability that b differs from a slope of 1. Traits with $p < 0.05$ are allometric and are indicated in bold. Table S2. Linear regression of all morphometric traits measured of the star-shaped pores of *Minibiotus sidereus* in relation to buccal tube length (BTL). Data log–log transformed. N = sample size, b = slope, a * = intercept, r^2 = coefficient of correlation, $t = (b - 1)/SE$ of b, p = probability that b differs from slope of 1. Traits with $p < 0.05$ are allometric and are indicated in bold.

Author Contributions: Conceptualization, F.A.-T.; methodology, A.D.-C., J.G.-R. and F.A.-T.; software, A.D.-C., J.G.-R. and F.A.-T.; validation, A.D.-C., F.A.-T. and E.A.R.; formal analysis, A.D.-C., J.G.-R. and F.A.-T.; investigation, A.D.-C., J.G.-R. and F.A.-T.; resources, F.A.-T. and E.A.R.; data curation, A.D.-C. and F.A.-T.; writing—original draft preparation, A.D.-C., J.G.-R. and F.A.-T.; review and editing, F.A.-T. and E.A.R.; visualization, A.D.-C., J.G.-R. and F.A.-T.; supervision, F.A.-T. and E.A.R.; project administration, F.A.-T. and E.A.R.; funding acquisition, F.A.-T. and E.A.R. All authors have read and agreed to the published version of the manuscript.

Funding: This research was funded by the SIP-IPN 20200591 (E.A.R), PAPIIT-UNAM IA201720 and CONACyT Fronteras de la Ciencia (139030) (F.A.-T.).

Institutional Review Board Statement: Not applicable.

Informed Consent Statement: Not applicable.

Data Availability Statement: The data are available in the supplementary materials.

Acknowledgments: We thank to Łukasz Kaczmarek and Giovanni Pilato for sharing images of *M. constellatus* and *M. sidereus*, respectively, for the refinement of our observations. We also thank Pedro Mercado Ruaro from the Laboratorio de Botánica Estructural, for phase contrast photographs, and María Berenit Mendoza Gárfias from Laboratorio de Microscopía Electrónica for the SEM micrography, both from the Laboratorio Nacional de Biodiversidad (LaNaBio), Instituto de Biología, Universidad Nacional Autónoma de México. We thank Joseph Heras for valuable comments on earlier versions of the manuscript. We thank Evelyn Martínez Méndez, who collaborated in using preliminary versions of the key and provide observations for its improvement. A.D.-C. (496686) and J.G.-R. (617368) were Consejo Nacional de Ciencia y Tecnología fellows. F.A.-T. and E.A.R. were members of Sistema Nacional de Investigadores-CONACyT.

Conflicts of Interest: The authors declare no conflict of interest.

References

1. Claxton, S.K. A revision of the genus *Minibiotus* Tardigrada: Macrobiotidae with descriptions of new species from Australia. *Rec. Aust. Mus.* **1998**, *50*, 125–160. [[CrossRef](#)]
2. Pilato, G.; Binda, M.G. A comparison of *Diphascon* (*D.*) *alpinum* Murray, 1906, *D.* (*D.*) *chilenense* Plate, 1889 and *D.* (*D.*) *pingue* Marcus, 1936 Tardigrada, and description of a new species. *Zool. Anz.* **1997**, *236*, 181–185.
3. Kaczmarek, Ł.; Michalczyk, Ł. The *Macrobiotus hufelandi* group (Tardigrada) revisited. *Zootaxa* **2017**, *4363*, 101–123. [[CrossRef](#)]
4. Morek, W.; Stec, D.; Gąsiorek, P.; Surmacz, B.; Michalczyk, Ł. *Milnesium tardigradum* Doyère, 1840: The first integrative study of interpopulation variability in a tardigrade species. *J. Zool. Syst. Evol. Res.* **2019**, *57*, 1–23. [[CrossRef](#)]

5. Gašiorek, P.; Morek, W.; Stec, D.; Blagden, B.; Michalczyk, Ł. Revisiting Calohypsibiidae and Microhypsibiidae: *Fractonotus* Pilato, 1998 and its phylogenetic position within Isohypsibiidae (Eutardigrada: Parachela). *Zoosystema* **2019**, *41*, 71–89. [[CrossRef](#)]
6. Binda, M.; Pilato, G.; Lisi, O. Remarks on *Macrobiotus furciger* Murray, 1906 and description of three new species of the furciger group (Eutardigrada, Macrobiotidae). *Zootaxa* **2005**, *1075*, 55–68. [[CrossRef](#)]
7. Fontoura, P.; Pilato, G. *Diphascaon* (*Diphascaon*) *faialense* sp. nov. a new species of Tardigrada Eutardigrada, Hypsibiidae from the Azores and a key to the species of the *D. pingue* group. *Zootaxa* **2007**, *1589*, 47–55. [[CrossRef](#)]
8. Kaczmarek, Ł.; Zawierucha, K.; Buda, J.; Stec, D.; Gawlak, M.; Michalczyk, Ł. An integrative redescription of the nominal taxon for the *Mesobiotus harmsworthi* group (Tardigrada: Macrobiotidae) leads to descriptions of two new *Mesobiotus* species from Arctic. *PLoS ONE* **2018**, *13*, e0204756. [[CrossRef](#)]
9. Pilato, G. Analisi di nuovi caratteri nello studio degli Eutardigradi. *Animalia* **1981**, *8*, 51–57.
10. Bertolani, R.; Rebecchi, L. A revision of the *Macrobiotus hufelandi* group (Tardigrada, Macrobiotidae), with some observations on the taxonomic characters of eutardigrades. *Zool. Scr.* **1993**, *22*, 127–152. [[CrossRef](#)]
11. Guidetti, R.; Bertolani, R. Tardigrade taxonomy: An updated check list of the taxa and a list of characters for their identification. *Zootaxa* **2005**, *845*, 1–46. [[CrossRef](#)]
12. Pilato, G.; Binda, G. Definition of families, subfamilies, genera and subgenera of the Eutardigrada, and keys to their identification. *Zootaxa* **2010**, *2404*, 1–54. [[CrossRef](#)]
13. Michalczyk, Ł.; Kaczmarek, Ł. The Tardigrada Register: A comprehensive online data repository for tardigrade taxonomy. *J. Limnol.* **2013**, *72*, 175–181. [[CrossRef](#)]
14. Pérez-Pech, W.A.; Anguas-Escalante, A.; Cutz-Pool, L.Q.; Guidetti, R. *Doryphoribius chetumalensis* sp. nov. (Eutardigrada: Isohypsibiidae) a new tardigrade species discovered in an unusual habitat of urban areas of Mexico. *Zootaxa* **2017**, *4344*, 347–352. [[CrossRef](#)]
15. Dastyh, H. The Tardigrada from Antarctic with descriptions of several new species. *Acta Zool. Cracov.* **1984**, *27*, 377–436.
16. Dastyh, H. *Macrobiotus ramoli* sp. nov., a new tardigrade species from the nival zone of the Ötztal Alps, Austria (Tardigrada). *Mitt. Hambg. Zool. Mus. Inst.* **2005**, *102*, 21–35.
17. Dastyh, H. A new tardigrade species of the genus *Ramazzottius* Binda & Pilato, 1986 (Tardigrada) from nival zone of the Mont Blanc (the Western Alps), with some morphometric remarks. *Mitt. Hambg. Zool. Mus. Inst.* **2006**, *103*, 33–45.
18. Pilato, G.; Binda, M.G.; Claxton, S. *Itaquason unguiculum* and *Itaquason cambewarrensense*: Two new species of eutardigrades from Australia. *N. Z. J. Zool.* **2002**, *29*, 87–93. [[CrossRef](#)]
19. Roszkowska, M.; Stec, D.; Ciobanu, D.A.; Kaczmarek, Ł. Tardigrades from Nahuel Huapi National Park (Argentina South America) with descriptions of two new Macrobiotidae species. *Zootaxa* **2016**, *4105*, 243–260. [[CrossRef](#)] [[PubMed](#)]
20. Blaxter, M.; Elsworth, B.; Daub, J. DNA taxonomy of a neglected animal phylum: An unexpected diversity of tardigrades. *Proc. R. Soc. Lond. B* **2004**, *271*, S189–S192. [[CrossRef](#)] [[PubMed](#)]
21. Jørgensen, A.; Møbjerg, N.; Kristensen, R.M. A molecular study of the tardigrade *Echiniscus testudo* (Echiniscidae) reveals low DNA sequence diversity over a large geographical area. *J. Limnol.* **2007**, *66*, 77–83. [[CrossRef](#)]
22. Cesari, M.; Bertolani, R.; Rebecchi, L.; Guidetti, R. DNA barcoding in Tardigrada: The first case study on *Macrobiotus macrocalix* Bertolani & Rebecchi 1993 (Eutardigrada, Macrobiotidae). *Mol. Ecol. Resour.* **2009**, *9*, 699–706. [[PubMed](#)]
23. Guidetti, R.; Schill, R.O.; Bertolani, R.; Dandekar, T.; Wolf, M. New molecular data for tardigrade phylogeny, with the erection of *Paramacrobiotus* gen. nov. *J. Zool. Syst. Evol. Res.* **2009**, *47*, 315–321. [[CrossRef](#)]
24. Guil, N.; Giribet, G. Fine scale population structure in the *Echiniscus blumi-canadensis* series (Heterotardigrada, Tardigrada) in an Iberian mountain range—When morphology fails to explain genetic structure. *Mol. Phylogenet. Evol.* **2009**, *51*, 606–613. [[CrossRef](#)]
25. Coughlan, K.; Stec, D. Two new species of the *Macrobiotus hufelandi* complex (Eutardigrada: Macrobiotidae) from Australia and India, with notes on their phylogenetic position. *EJT* **2019**, *573*, 1–38. [[CrossRef](#)]
26. Nelson, D.R.; Adkins, R.; Guidetti, R.; Roszkowska, M.; Grobys, D.; Kaczmarek, Ł. Two new species of Tardigrada from moss cushions (*Grimmia* sp.) in a xerothermic habitat in northeast Tennessee (USA, North America), with the first identification of males in the genus *Viridiscus*. *PeerJ* **2020**, *8*, e10251. [[CrossRef](#)] [[PubMed](#)]
27. Stec, D.; Kristensen, R.M.; Michalczyk, Ł. An integrative description of *Minibiotus ioculator* sp. nov. from the Republic of South Africa with notes on *Minibiotus pentannulatus* Londoño et al., 2017 (Tardigrada: Macrobiotidae). *Zool. Anz.* **2020**, *286*, 117–134. [[CrossRef](#)]
28. Kayastha, P.; Berdi, D.; Mioduchowska, M.; Gawlak, M.; Łukasiewicz, A.; Goldyn, B.; Kaczmarek, Ł. Some tardigrades from Nepal (Asia) with integrative description of *Macrobiotus wandae* sp. nov. (Macrobiotidae: Hufelandi group). *Annal. Zool.* **2020**, *70*, 121–142. [[CrossRef](#)]
29. Kihm, J.H.; Kim, S.; McInnes, S.; Zawierucha, K.; Rho, H.S.; Kang, P.; Park, T.S. Integrative description of a new *Dactylobiotus* (Eutardigrada: Parachela) from Antarctica that reveals an intraspecific variation in tardigrade egg morphology. *Sci. Rep.* **2020**, *10*, 9122. [[CrossRef](#)]
30. Tumanov, D.V. Integrative redescription of *Hypsibius pallidoides* Pilato et al., 2011 (Eutardigrada: Hypsibioidea) with the erection of a new genus and discussion on the phylogeny of Hypsibiidae. *EJT* **2020**, *681*, 1–37.
31. Pilato, G. Revision of the genus *Diphascaon* Plate, 1889, with remarks on the subfamily Itaquasconinae (Eutardigrada, Hypsibiidae). In *Biology of Tardigrades. Selected Symposia and Monographs*; Bertolani, R., Ed.; U.Z.I. Mucchi Editore: Modena, Italy, 1987; Volume 1, pp. 337–357.

32. Dastych, G.; Thaler, K. The tardigrade *Hebesuncus conjungens* (Thulin, 1911) in the Alps, with notes on morphology and distribution (Tardigrada). *Entomol. Mitt. Zool. Hambg.* **2002**, *14*, 83–94.
33. Kaczmarek, Ł.; Cytan, J.; Zawierucha, K.; Diduszko, D.; Michalczyk, Ł. Tardigrades from Peru (South America), with descriptions of three new species of Parachela. *Zootaxa* **2014**, *3790*, 357–379. [[CrossRef](#)] [[PubMed](#)]
34. Beasley, C.W.; Kaczmarek, Ł.; Michalczyk, Ł. *Doryphoribius mexicanus*, a new species of Tardigrada Eutardigrada: Hypsibiidae from Mexico North America. *Biol. Soc. Wash.* **2008**, *121*, 34–40. [[CrossRef](#)]
35. Fontoura, P.; Morais, P. Assessment of traditional and geometric morphometrics for discriminating cryptic species of the *Pseudechiniscus suillus* complex (Tardigrada, Echiniscidae). *J. Zool. Syst. Evol. Res.* **2011**, *49*, 26–33. [[CrossRef](#)]
36. Gąsiorek, P.; Stec, D.; Morek, W.; Michalczyk, Ł. An integrative redescription of *Echiniscus testudo* (Doyere, 1840), the nominal taxon for the class Heterotardigrada (Ecdysozoa: Panarthropoda: Tardigrada). *Zool. Anz.* **2017**, *270*, 107–122. [[CrossRef](#)]
37. Moreno-Talamantes, A.; Roszkowska, M.; García-Aranda, M.A.; Flores-Maldonado, J.J.; Kaczmarek, Ł. Current knowledge on Mexican tardigrades with a description of *Milnesium cassandrae* sp. nov. (Eutardigrada: Milnesiidae) and discussion on the taxonomic value of dorsal pseudoplates in the genus *Milnesium* Doyère, 1840. *Zootaxa* **2019**, *4691*, 501–524. [[CrossRef](#)] [[PubMed](#)]
38. Gąsiorek, P.; Stec, D.; Morek, W.; Michalczyk, Ł. An integrative redescription of *Hypsibius dujardini* Doyère, 1840, the nominal taxon for Hypsibioida Tardigrada: Eutardigrada. *Zootaxa* **2018**, *44151*, 45–75. [[CrossRef](#)]
39. Pilato, G.; Costa, G.; Conti, E.; Binda, M.G.; Lisi, O. Morphometric analysis of some metric characters of two *Macrobiotus* species (Eutardigrada, Macrobiotidae). *J. Limnol.* **2007**, *66*, 26–32. [[CrossRef](#)]
40. Zawierucha, K.; Stec, D.; Lachowska-Cierlik, D.; Takeuchi, N.; Michalczyk, Ł. High mitochondrial diversity in a new water bear species (Tardigrada: Eutardigrada) from mountain glaciers in Central Asia, with the erection of a new genus *Cryoconius*. *Ann. Zool.* **2018**, *68*, 179–201. [[CrossRef](#)]
41. Stec, D.; Gąsiorek, P.; Morek, W.; Kosztyla, P.; Zawierucha, K.; Michno, K.; Kaczmarek, Ł.; Prokop, Z.M.; Michalczyk, Ł. Estimating optimal sample size for tardigrade morphometry. *Zool. J. Linn. Soc.* **2016**, *178*, 776–784. [[CrossRef](#)]
42. Stec, D.; Smolak, R.; Kaczmarek, Ł.; Michalczyk, Ł. An integrative description of *Macrobiotus paulinae* sp. nov. (Tardigrada: Eutardigrada: Macrobiotidae: Hufelandi group) from Kenya. *Zootaxa* **2015**, *4052*, 501–526. [[CrossRef](#)] [[PubMed](#)]
43. Roszkowska, M.; Gawlak, M.; Draga, M.; Kaczmarek, Ł. Two new species of Tardigrada from Ecuador (South America). *Zootaxa* **2019**, *4545*, 511–530. [[CrossRef](#)] [[PubMed](#)]
44. Ramazzotti, G.; Maucci, W. *Il Phylum Tardigrada*. Terza edizione riveduta e corretta. *Mem. Istituto Ital. Idrobiol. Dott. Marco Marchi* **1983**, *41*, 1–1012.
45. Stec, D.; Morek, W.; Gąsiorek, P.; Michalczyk, Ł. Unmasking hidden species diversity within the *Ramazzottius oberhaeuseri* complex, with an integrative redescription of the nominal species for the family Ramazzottiidae (Tardigrada: Eutardigrada: Parachela). *Syst. Biodivers.* **2018**. [[CrossRef](#)]
46. Bartylak, T.; Kulpa, A.; Grobys, D.; Kepel, M.; Kepel, A.; Kmita, H.; Gawlak, M.; Grabinski, W.; Roszkowska, M.; Kaczmarek, Ł. Variability of *Echiniscus tristis* Gąsiorek & Kristensen, 2018—is morphology sufficient for taxonomic differentiation of Echiniscidae? *Zootaxa* **2019**, *407*, 1–24.
47. Pilato, G.; Binda, M.G.; Lisi, O. Three new species of eutardigrades from the Seychelles. *New Zealand J. Zool.* **2006**, *33*, 39–48. [[CrossRef](#)]
48. Michalczyk, Ł.; Kaczmarek, Ł. *Minibiotus constellatus*, new species of Tardigrada from Peru (Eutardigrada: Macrobiotidae). *Genus* **2003**, *14*, 295–305.
49. Pilato, G.; Binda, M.G.; Lisi, O. Remarks on some species of tardigrades from South America with description of *Minibiotus sidereus* n. sp. *Zootaxa* **2003**, *195*, 1–8. [[CrossRef](#)]
50. Dueñas-Cedillo, A.; Martínez-Méndez, E.; García-Román, J.; Armendáriz-Toledano, F.; Ruiz, E.A. Tardigrades from Iztaccíhuatl Volcano (Trans-Mexican Volcanic Belt), with the Description of *Minibiotus citlalium* sp. nov. (Eutardigrada: Macrobiotidae). *Diversity* **2020**, *12*, 271. [[CrossRef](#)]
51. Londoño, R.; Daza, A.; Lisi, O.; Quiroga, S. New species of waterbear *Minibiotus pentannulatus* (Tardigrada: Macrobiotidae) from Colombia. *Rev. Mex. Biodivers.* **2017**, *88*, 807–814. [[CrossRef](#)]
52. Michalczyk, Ł.; Kaczmarek, Ł. *Minibiotus eichhorni* sp. nov., a new species of eutardigrade (Eutardigrada: Macrobiotidae) from Peru. *Ann. Zool.* **2004**, *54*, 673–676.
53. Chim, C.K.; Tan, K.S. Recognition of individual knobby sea stars *Protoreaster nodosus* (L., 1758) using aboral surface characteristics. *J. Exp. Mar. Biol. Ecol.* **2012**, *430*, 48–55. [[CrossRef](#)]
54. Rohlf, F.J. *TPS Dig v 2.31*; Department of Ecology and Evolution, State University of New York: Stony Brook, NY, USA, 2017. Available online: <http://life.bio.sunysb.edu/morph/> (accessed on 1 May 2021).
55. Shapiro, S.S.; Wilk, M.B. An analysis of variance test for normality (complete samples). *Biometrika* **1965**, *52*, 591–611. [[CrossRef](#)]
56. Guillaumin, M. Etude biometrique des populations naturelles de *P. Carlivae* Rbr et *P. Ciasii* Rbr (Lep. Hesperidae). I Estimation du taux de chevauchement des distributions statistiques de deux populations en relation avec la notion de distance taxonomique. *Arch. Zool. Exp. Gen.* **1972**, *115*, 505–548.
57. Zar, J.H. *Biostatistical Analysis*, 5th ed.; Prentice Hall: Englewood Cliffs, NJ, USA, 2010; pp. 1–929.
58. Bartels, P.J.; Nelson, D.R.; Exline, R.P. Allometry and the removal of body size effects in the morphometric analysis of tardigrades. *J. Zool. Syst. Evol. Res.* **2011**, *49*, 17–25. [[CrossRef](#)]

59. Hammer, Ø.; Harper, D.A.T.; Ryan, P.D. PAST: Paleontological statistics software package for education and data analysis. *Palaeontol. Electron.* **2001**, *4*, 9.
60. Legendre, P.; Legendre, L. *Numerical Ecology: Developments in Environmental Modeling 20*, 2nd ed.; Elsevier B.V.: Amsterdam, The Netherlands, 1998.
61. Kristensen, R.M. Generic revision of the Echiniscidae (Heterotardigrada), with a discussion of the origin of the family. In *Biology of Tardigrades*; Bertolani, R., Ed.; Selected Symposia and Monographs; U.Z.I. Mucchi Editore: Modena, Italy, 1987; pp. 261–335.
62. Fontoura, P.; Bartels, P.J.; Jørgensen, A.; Kristensen, R.M.; Hansen, J.G. A dichotomous key to the genera of the Marine Heterotardigrades (Tardigrada). *Zootaxa* **2017**, 1–45. [[CrossRef](#)]
63. Hansen, J.G.; Gallo D'Addabbo, M.; De Zio Grimaldi, S. A comparison of morphological characters within the genus *Rhomborctus* (Tardigrada: Heterotardigrada) with the description of two new species. *Zool. Anz.* **2003**, *242*, 83–96. [[CrossRef](#)]
64. Tumanov, D.V. Analysis of non-morphometric morphological characters used in the taxonomy of the genus *Pseudechiniscus* (Tardigrada:Echiniscidae). *Zool. J. Linn. Soc.* **2020**, *188*, 753–775.
65. Vecchi, M.; Cesari, M.; Bertolani, R.; Jonsson, K.I.; Rebecchi, L.; Guidetti, R. Integrative systematic studies on tardigrades from Antarctica identify new genera and new species within Macrobiotidea and Echiniscoidea. *Invertebr. Syst.* **2016**, 303–322. [[CrossRef](#)]
66. Cesari, M.; Montanari, M.; Reinhardt, M.K.; Bertolani, R.; Guidetti, R.; Rebecchi, L. An integrated study of the biodiversity within the *Pseudechiniscus suillus-facettalis* group (Heterotardigrada: Echiniscidae). *Zool. J. Linn. Soc.* **2020**, *188*, 717–732. [[CrossRef](#)]
67. Gąsiorek, P.; Voncina, K.; Zajac, K.; Michalczyk, L. Phylogeography and morphological evolution of *Pseudechiniscus* (Heterotardigrada: Echiniscidae). *Sci. Rep.* **2021**, *11*, 1–16. [[CrossRef](#)]
68. Nelson, D.R.; Marley, N.J. The biology and ecology of lotic Tardigrada. *Freshw. Biol.* **2000**, *44*, 93–109. [[CrossRef](#)]
69. Gąsiorek, P.; Stec, D.; Morek, W.; Michalczyk, L. Deceptive conservatism of claws: Distinct phyletic lineages concealed within Isohypsibioidea (Eutardigrada) revealed by molecular and morphological evidence. *Contrib. Zool.* **2019**, *88*, 78–132. [[CrossRef](#)]
70. Guidetti, R.; Rebecchi, L.; Bertolani, R. Cuticle structure and systematics of the Macrobiotidae (Tardigrada, Eutardigrada). *Acta Zool.* **2000**, *81*, 27–36. [[CrossRef](#)]
71. Bertolani, R.; Guidetti, R.; Marchioro, T.; Altiero, T.; Rebecchi, L.; Cesari, M. Phylogeny of Eutardigrada: New molecular data and their morphological support lead to the identification of new evolutionary lineages. *Mol. Phylogenet. Evol.* **2014**, *76*, 110–126. [[CrossRef](#)] [[PubMed](#)]
72. Stec, D.; Krzywanski, L.; Zawierucha, K.; Michalczyk, L. Untangling systematics of the *Paramacrobotus areolatus* species complex by an integrative redescription of the nominal species for the group, with multilocus phylogeny and species delineation in the genus *Paramacrobotus*. *Zool. J. Linn. Soc.* **2020**, *188*, 694–716. [[CrossRef](#)]
73. Muster, C.; Michalik, P. Cryptic diversity in ant-mimic *Micaria* spiders (Araneae, Gnaphosidae) and a tribute to early naturalists. *Zool. Scr.* **2020**, *49*, 197–209. [[CrossRef](#)]
74. Cai, R.; Prior, T.; Lawson, B.; Cantalapiedra-Navarrete, C.; Palomares-Rius, J.E.; Castillo, P.; Archidona-Yuste, A. An integrative taxonomic study of the needle nematode complex *Longidorus goodeyi* Hooper, 1961 (Nematoda: Longidoridae) with description of a new species. *Eur. J. Plant. Pathol.* **2020**, *158*, 59–81. [[CrossRef](#)]
75. Cid-Muñoz, R.; Cibrián-Tovar, D.; Valadez-Moctezuma, E.; Estrada-Martinez, E.; Armendariz-Toledano, F. Biology and Life Stages of Pine Spittle Bug *Ocoaxo assimilis* Walker (Hemiptera: Cercopidae). *Insects* **2020**, *11*, 96. [[CrossRef](#)] [[PubMed](#)]
76. Moly de Peluffo, M.C.; Paluffo, J.R.; Rocha, A.M.; Doma, I.L. Tardigrade distribution in a medium-sized city of central Argentina. *Hydrobiologia* **2006**, *558*, 141–150. [[CrossRef](#)]